IEEE Access
Multidisciplinary | Rapid Review | Open Access Journal

Received April 16, 2018, accepted May 23, 2018, date of publication June 19, 2018, date of current version August 7, 2018.

Digital Object Identifier 10.1109/ACCESS.2018.2846290

Estimating Dynamic Motion Parameters With an Improved Wavelet Thresholding and Inter-Scale Correlation

YUANHUI WANG[1], (Member, IEEE), BO ZHANG[1], FUGUANG DING[1], AND HONGLIANG REN[2,3], (Senior Member, IEEE)

[1]College of Automation, Harbin Engineering University, Harbin 150001, China
[2]Department of Biomedical Engineering, National University of Singapore, Singapore 117575
[3]National University of Singapore Suzhou Research Institute, Suzhou 215123, China

Corresponding authors: Fuguang Ding (dingfuguang@hrbeu.edu.cn) and Hongliang Ren (ren@nus.edu.sg)

This work was supported in part by the Hovercraft Motion Simulation System Project and in part by the NUSRI China Jiangsu Province under Grants BK20150386 and BE2016077.

ABSTRACT With the challenging noisy measurements, the maneuvering safety and comfort level of hovercraft navigation can be significantly increased by accurate motion parameter estimation. Because traditional hard/soft thresholding schemes have discontinuities and deviation shortcomings, an improved wavelet thresholding method is proposed to smooth and estimate the dynamic motion parameters. Then, an inter-scale correlation method is introduced to improve the accuracy of judgment of the wavelet coefficients near the threshold. The newly improved wavelet thresholding and inter-scale correlation scheme can increase the adaptability of the estimator function and improve the accuracy of judgment of wavelet coefficients. Afterwards, a series of numerical simulation experiments are carried out by using four benchmark signals with three different noise levels. Compared with traditional hard/soft thresholding and semi-soft thresholding methods, the proposed improved parameter estimation scheme has a great advantage in denoising the signal noise and reducing the peak interference and the error between decomposition signal and the original signal. Finally, the proposed improved parameter estimation scheme was applied to a certain hovercraft in sea trial. Representatively, some important safety and comfort indicator parameters are selected from actual hovercraft motion measurements to verify the effect of the proposed scheme. From the data analysis, it is shown that the improved scheme behaves an outstanding performance in denoising and estimating for practical application, which improves the safety and comfort of navigation. Otherwise, the effective estimation of indicator parameters will make the further active control be available to assure maneuvering safety and comfort level of hovercraft navigation.

INDEX TERMS Motion parameters, wavelet transform, thresholding function, inter-scale correlation, denoise.

I. INTRODUCTION

A hovercraft, known as an air-cushion vehicle or ACV, is a craft capable of traveling over land, water, mud, ice, and other surfaces. Noise is the biggest challenge faced by hovercraft designers and builders. A well-known limit is the so-called ''cobblestone effect'', a resonance phenomenon, which is due to the interaction between the ship body and the air cushion dynamics, excited by the incoming waves. Considering the cobblestone phenomenon, dynamics and control should be studied carefully in hovercraft design step.

Meanwhile, due to high speed, small water resistance, and poor rotation ability, the hovercraft is always with poor maneuverability. Any inappropriate or wrong operation may cause a heavy accident. To improve the maneuvering safety and comfort level of the hovercraft navigation, some researchers were working on seeking a better controller design, such as Sira-Ramirez [1] and Seguchi and Ohtsuka [2]. Alternatively, the accurate motion-parameter estimation will become another good choice. Caused by hovercraft noise and vibration, the sensor signals of hovercraft will suffer distortions. Attention is drawn to

the fact that actual measurements reveal that this noise is appreciably higher than would be expected from theoretical prediction. Without effective signal processing, the subsequent dynamic control operations will be inaccurate and error-prone, which may cause accident or failure. Therefore, it is essential to denoise and estimate the dynamic motion parameters.

Although there are few studies on the estimation of hovercraft application, parameter estimation has attracted wide attention in other areas. Yin *et al.* [3] used locally weighted total PLS monitoring approach to monitor the quality of the wastewater treatment. Xie *et al.* [4] proposed a method called advanced partial least squares (APLS) to efficiently distinguish the key performance indicator (KPI) and verify through the Tennessee Eastman(TE) benchmark process. At the same time, a variety of filtering methods were introduced to denoise, for example, the median filter [5], FFT thresholding [6], adaptive filtering [7], FIR filtering [8], intelligent particle filter [9], etc. These conventional filtering methods can effectively remove discrete spectral interferences(DSI) and colored noise, but cannot denoise white Gaussian noise [10]. Moreover, when the signal involves transient impulses with a sharp edge and of very short duration, it is difficult to eliminate the noise signal by linear filters [11]. Moreover, the linear filter will not be used when the signal overlaps with the noise in many different frequency bands [12]. These disadvantages of linear filters tend to disable the noise and useful signal component identification and lead to bad denoising results. To enhance linear filter effects, the FIR filter-based noise reduction techniques in the transform domain have been investigated [13]. However, because of the transformation is still linear, the filter still has worse performance.

To overcome difficulties, the wavelet transform theory that maintains both time domain and frequency domain information is proposed and widely used in the denoising technology [14], [15]. Generally, there are three main denoising algorithms based on wavelet transform: wavelet coefficients modulus maxima method, wavelet correlation method, and wavelet thresholding method. Because the thresholding method is simple and effective, it is widely used once proposed by Donoho and Johnstone [16]. Among the wavelet transform thresholding methods, the hard/soft thresholding techniques are the conventional thresholding methods [6]. Due to the main idea of the method being the noise elimination by thresholding wavelet coefficients, so the thresholding function and threshold are important factors that affect the denoising performance. However, the traditional hard thresholding exhibits some discontinuities and is more sensitive to little changes of a signal. As for soft thresholding, it induces the deviation in the process of wavelet reconstruction. To overcome these shortcomings, Breiman's nonnegative garrote method was added into the Wave Shrink and the simulation results show that this method is more stable and offers smaller range than the hard and soft shrinkage [17]. To *et al.* [18] proposed a comparison research between the wavelet-based techniques with soft/hard wavelet thresholding and the empirical Bayes (EB) method was carried out. The EB method outperformed the others in general because the wavelet representation is not sparse at the coarsest levels. Bacchelli and Papi [19] used two new filters that are a piecewise quadratic and an exponential function. Ting-Hua *et al.* [20] used sigmoid function as wavelet thresholding function to improve the denoising performance. But the function is not adaptive. Ray *et al.* [11] proposed a new nonlinear threshold function for denoising PD (partial discharge) signal using wavelet transform technique. A field-detected signal was tested and the denoised signal indicated that the method is efficient for this application. Wang [21] put forward a new wavelet thresholding function based on hyperbolic tangent function was used and simulation results show that the proposed function can achieve better denoising effect. Lu *et al.* [22] introduced the logarithmic function of the layer number of wavelet decomposition to put forward a new threshold function. Hussein *et al.* [23] used a denoising scheme called histogram-based thresholding estimation (HBTE) to remove the noise from the partial discharge signal effectively. Lee and Kim [24] proposed hard thresholding rule and Visushrink threshold value to eliminate the noise of DCV (discharging/charging voltage).

In this article, the main contributions are highlighted as follows:

1) To overcome the discontinuities and deviation shortcomings of traditional hard/soft thresholding methods, a new wavelet thresholding function and an improved threshold are proposed to improve the denoising and estimating effects and increase the adaptability of the estimator function.
2) Inter-scale correlation is introduced into the above new wavelet threshold method to improve the accuracy of judgment of the wavelet coefficients near the threshold.
3) A series of numerical simulation experiments are carried out by using four benchmark signals with three different noise levels. Compared with traditional hard/soft thresholding and semi-soft thresholding methods, the proposed improved parameter estimation method has a great advantage in denoising the signal noise and reducing the peak interference and the error between decomposition signal and the original signal.
4) The important safety and comfort indicator parameters for dynamic navigation are defined, which are selected from certain actual hovercraft motion measurements to verify the effect of the proposed improved parameter estimation scheme in practical application. It behaves an outstanding performance in denoising and estimating, which improves the maneuvering safety and comfort level of dynamic navigation

The structure of this article is the following: first, the theory of traditional hard/soft thresholding summarized in Section 2. Second, a new wavelet thresholding function, an improved threshold and the method of inter-scale correlation based on wavelet transform are introduced in Section 3. Third,

a numerical simulation cases study using four benchmark signals are carried out to verify the effectiveness of the new denoising scheme in Section 4. Fourth, the thresholding scheme to smooth the sea trial measurements of hovercraft motion parameters is presented to behave a better denoising performance in Section 5. Finally, conclusions are drawn in Section 6.

II. TRADITIONAL WAVELET THRESHOLDING DENOISING

Assume the noise signal is as follows:

$$y_i = x_i + e_i \tag{1}$$

where y_i is the noised signal, x_i is the original signal and e_i is the noise that is independently distributed according to a zero-mean Gaussian distribution, $N(0, \sigma^2)$ [25]. In the signal y_i, obviously, some valuable information of the original signal is destroyed and the noise should be removed. In discrete wavelet transform (DWT), the signal y_i is passed through a series of low-pass and high-pass filters with various frequencies. Approximated coefficient and wavelet coefficient can be expressed as follows:

$$\begin{aligned} c_{j,k} &= \sum c_{j-1,n} h^*(n-2k) \\ d_{j,k} &= \sum d_{j-1,n} g^*(n-2k) \end{aligned} \tag{2}$$

where $c_{j,k}$ is approximated coefficient, $d_{j,k}$ is wavelet coefficient. $h^*(n-2k)$ and $g^*(n-2k)$ are decomposed low-pass and high-pass filter, respectively. Wavelet reconstruction is:

$$c_{j-1,k} = \sum_k c_{j,n} \bar{h}^*(n-2k) + \sum_k d_{j,n} \bar{g}^*(n-2k) \tag{3}$$

where, $\bar{h}^*(n-2k)$ and $\bar{g}^*(n-2k)$ are reconstructed low-pass and high-pass filters.

By thresholding observed wavelet coefficients representing noise, a smooth estimate of the underlying can be obtained [26], [27]. The traditional wavelet thresholding denoising procedure can be described as follows:

1) Select the wavelet basis and determine the maximum number of signal decomposition level.
2) Use discrete wavelet transform (DWT) to decompose the signal and get wavelet coefficient and approximated coefficient of each decomposition level j.
3) Apply the thresholding function and the calculated threshold to discard the wavelet coefficient of null value and get estimated wavelet coefficient.
4) Reconstruct the signal using approximated coefficient and estimated wavelet coefficient by inverse discrete wavelet transform (IDWT) to acquire a denoised signal.

In the wavelet thresholding technique, thresholding function has a major effect on the quality of signal [28]. The traditional thresholding functions are hard thresholding and soft thresholding. The hard thresholding used by Donoho [10], [16] is considered as ''keep or kill''. Sometimes, pure noise coefficients may pass the hard thresholding and appear as annoying ''blips'' in the output image. It can be defined as follows:

$$\widehat{\omega}_{j,k} = \begin{cases} \omega_{j,k}, & for\ (|\omega_{j,k}| \geq T) \\ 0, & otherwise \end{cases} \tag{4}$$

where $\hat{w}_{j,k}$, and $w_{j,k}$ are the shrink and original wavelet coefficients and T is the threshold.

The soft thresholding also used by Donoho is considered as ''shrink or kill'' and can overcome the false structures in the hard thresholding. However, the results of this function lose a part of high-frequency coefficients above the threshold. It is defined as follows:

$$\widehat{\omega}_{j,k} = \begin{cases} \mathrm{sgn}(\omega_{j,k})(|\omega_{j,k}| - T) & for(|\omega_{j,k}| \geq T) \\ 0 & otherwise \end{cases} \tag{5}$$

Besides thresholding function, threshold T is another important element to directly influence the result of denoising by thresholding function. Among the existing methods, the most popular one is the universal threshold [11]. It is defined as follows:

$$T = \sigma\sqrt{2\ln N} \tag{6}$$

Where, N denotes the length of a signal; σ represents the noise standard deviation, which can be estimated from the median of the detail coefficients [20]:

$$\sigma = \frac{|median(\omega_{j,k})|}{0.6745} \tag{7}$$

III. THE IMPROVED THRESHOLDING METHOD

A. NEW THRESHOLDING FUNCTION

In the traditional thresholding approaches, there are some shortcomings. For example, in the hard thresholding process, the denoised wavelet coefficients may exhibit discontinuity at the location of threshold T and it may result in Gibbs shock [20]. In the soft thresholding method, the coefficients may have a constant bias compared with the original coefficients, which makes the reconstructed signal different from the original signal. In order to improve the denoising performance, the semisoft threshold function [29] has been shown in the formula:

$$\widehat{\omega}_{j,k} = \begin{cases} \mathrm{sgn}(\omega_{j,k})(|\omega_{j,k}| - \alpha T) & for(|\omega_{j,k}| \geq T) \\ 0 & otherwise \end{cases} \tag{8}$$

Among the semisoft function, the value of α is taken between 0 and 1. Even if the result of semisoft threshold function is better than hard and soft threshold function, the value of α is fixed. So the new proposed thresholding function should satisfy the following assumptions:

- The input-output curve of the function based thresholding scheme should be continuous and smooth to reduce the oscillation phenomenon and the Gibbs shock.
- Reduce the constant bias of the soft thresholding and retain the signal edge details.

The new improved adaptive threshold function that meets the above requirements is proposed in this paper defined as:

$$\widehat{\omega}_{j,k} = \begin{cases} \mathrm{sgn}(\omega_{j,k})(\left|\omega_{j,k}\right| - \dfrac{e^{(\beta * T)}}{e^{(\beta * \left|w_{j,k}\right|)}} T) & for(\left|\omega_{j,k}\right| \geq T) \\ 0 & otherwise \end{cases} \tag{9}$$

Where, β is a non-negative number. The new function is based on the semisoft threshold function, which makes the parameter α adaptive. When the value of $|w_{j,k}|$ is smaller, $\alpha \to 1$, the function has the characteristics of soft threshold function. It can reduce Gibbs shock. Else if $|w_{j,k}|$ is bigger, $\alpha \to 0$, the function has the characteristics of hard threshold function. It can retain edge details. So the adaptive function is obtained by comparing $w_{j,k}$ and T. The value of β also affects threshold function characteristics. When $\beta \to 0$ and $\beta \to \infty$, this function approximately transfers into the soft thresholding function and hard thresholding function, respectively:

$$\lim_{\beta \to 0} \widehat{\omega}_{j,k} \approx \omega_{j,k} \tag{10}$$

$$\lim_{\beta \to \infty} \widehat{\omega}_{j,k} \approx sgn(\omega_{j,k})(\left|\omega_{j,k}\right| - T) \tag{11}$$

Obviously, the new thresholding function is a compromise derived from the traditional thresholdings approachees. Therefore, the value of β in the new threshold function should take a proper value. After given a suitable β, the new threshold function can be treated differently depending on the size of the wavelet coefficients. When the value of $|w_{j,k}|$ is smaller, the function has the characteristics of the soft threshold, if $|w_{j,k}|$ is bigger, the function has the characteristics of hard threshold function. The comparison among soft, hard, semisoft and proposed new thresholding function is illustrated in Fig.1, where $\alpha = 0.6$, $\beta = 2$, $-1.5 \leq w_{j,k} \leq 1.5$, $T = 0.5$.

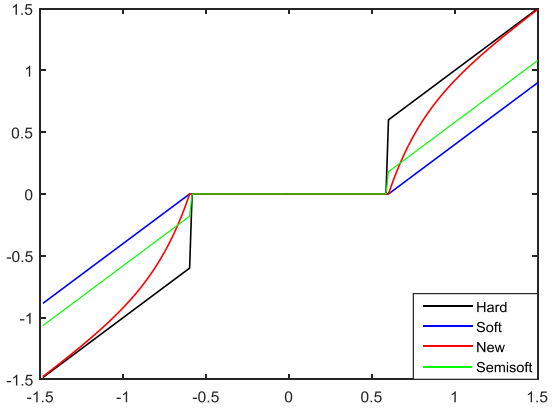

FIGURE 1. The comparison among soft, hard, semi-soft and new thresholding function.

B. THRESHOLD ESTIMATION

In addition to the thresholding function, a rational threshold value is another parameter that directly affects the denoising effects. The threshold is mainly composed of wavelet subband energy and noise variance of signal that is measured from the observed data. The estimation of an appropriate threshold value makes a difference between the wavelet coefficient of noise and that of the original signal [30]. If the threshold is small, the noise will not be completely filtered out. Moreover, if the threshold is large, part of the real signal will be filtered out with the noise, which will lead to the outcome bias. Since the wavelet coefficient of noise decreases with the increase of the scale, the threshold should be different when the scale changes. To overcome the disadvantage that the universal threshold has of not changing with the decomposition scale, the threshold is proposed to account for the different scales of wavelet coefficients [22]:

$$T = \sigma \sqrt{2 \ln N} / \log_2(1 + j) \tag{12}$$

Where, j is the decomposition scale. The improved threshold maintains the length of signal N and the noise standard deviation σ of the universal threshold, at the same time, add the scale in the denominator. The improved threshold is more adaptive to the noise, signal characteristics and increases the threshold practical value.

C. WAVELET COEFFICIENT INTER-SCALE CORRELATION

By adequately using wavelet thresholding method, the white Gaussian noise can be efficiently filtered out by subtracting a threshold from noisy wavelet coefficients [31]. However, filtering by wavelet threshold suffers from residual noise and signal distortion. To improve the accuracy of signal denoising, the wavelet correlation theory is introduced to judge the wavelet coefficients that near the threshold T.

In the process of wavelet decomposition, the signal is decomposed into approximation coefficients and wavelet coefficients that represent the signal details. The signal power and noise power are broken down into various scales by multi-scale orthogonal discrete wavelet transform [32]. The usual wavelet transform denoising methods make full use of these characteristics that the point of discontinuity has good local property characteristic in every scales of the wavelet coefficients. The noise energy is focused on small-scale wavelet coefficients that rapid attenuation with the increase of scales. However, the situation correlation of wavelet coefficients in the residual still exists, especially between the adjacent decomposition scales. In [33], it pointed out that the wavelet coefficients in each scale have strong relevance and its correlation is more obvious near the point of discontinuity. In contrast, the wavelet coefficients corresponding to the noise not have the obvious correlation between the scales. On the basis of it, SSNF (Spatially selective noise filtration) was proposed [34]. The main idea of this method is the direct spatial correlation of the wavelet transform at several adjacent scales and take correlation filter processing by multiplying adjacent scales wavelet coefficients.

In the SSNF, first, assume the maximum scale of the wavelet decomposition is J. $Wf(j,k)$ represents the wavelet coefficient of noised signal f at the position k and the scale j. The adjacent scales correlation coefficient $Corr_L(j,k)$ is defined as [35]:

$$Corr_L(j,k) = \prod_{i=0}^{L-1} Wf(j+i,k) \tag{13}$$

Where L is the number of scales involved in the direct multiplication. Usually, L is 2.Then, in order to compare the correlation coefficient and wavelet coefficient, a normalization of the correlation coefficient is defined as [34]:

$$NCorr_L(j,k) = Corr_L(j,k)\sqrt{\frac{Pw(j)}{PCorr(j)}} \quad k = 1, 2, \cdots, N \tag{14}$$

$$P_{Corr_2}(j) = \sum_{k=1}^{N} Corr_2(j,k)^2 \tag{15}$$

$$P_W(j) = \sum_{k=1}^{N} Wf(j,k)^2 \tag{16}$$

By comparing the $Wf(j,k)$ and the normalization of correlation coefficient to distinguish the effective coefficient from invalid coefficient. In the SSNF, the iterative operation is needed in the following steps and it is a large amount of calculation. However, in this paper, the wavelet coefficient correlation is the auxiliary in the denoising algorithm. On the one hand, the amount of calculation is not very large; on the other hand, the accuracy requirements of scales correlation estimation is not very high. The correlation coefficients of the two-dimensional images are converted to the correlation coefficients representing the one-dimensional signals. The new correlation K is defined as:

$$K(J,k) = \frac{\max w(J,k)}{\min w(J,k)} \tag{17}$$

Where J is the decomposition scale, n is the position. $\max w(J,k)$ is the maximum among $w_k^1, w_k^2, \cdots w_k^J$ them. $\min w(J,k)$ is the minimum among them. When K(J,k)$\in[1,\gamma]$, it means the correlation of wavelet coefficients is strong and the signal is useful. Besides, it represents the correlation of wavelet coefficients is weak and the signal is the noise. When γ is nearly 1, the difference of $\max w(J,k)$ and $\min w(J,k)$ is small and the inter-scale correlation estimation is strict. It will cause more valued wavelet coefficient regression. If γ is too large, it will lead to choosing noise coefficient as a useful signal, which cannot achieve the goal of effective denoising. In this paper, when selecting the value of γ, the strict rule is chosen to ensure the denoising effect.

In the process of calculating $K(J,k)$, the wavelet coefficients of different scales should expand into the same size. Because of each coefficient of the rough layer corresponds to two coefficients of the same sub-band in the adjacent fine layers, the copying and expansion method is 1*2. When decomposition layers increases, the expansion of coefficient is harder. Therefore, the method of scales correlation estimation is suitable for the situation that the decomposition level is not too large. The copying and expansion method is shown in Fig. 2.

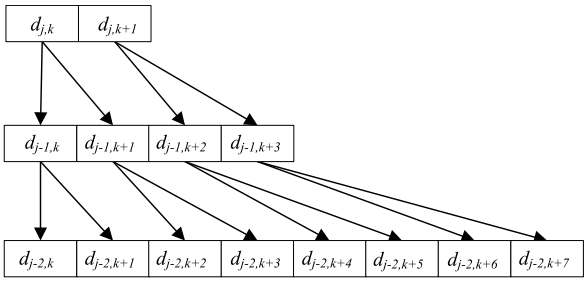

FIGURE 2. The copying and expansion method of wavelet coefficient in the level of *j*.

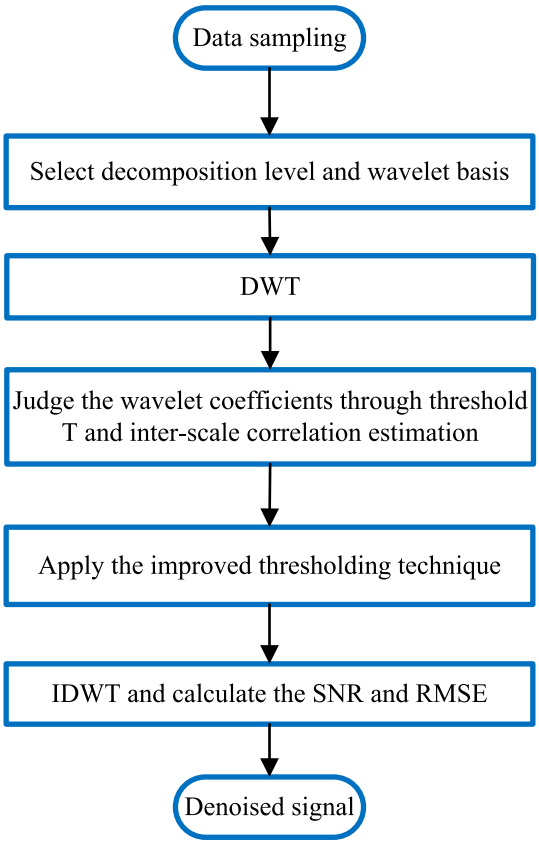

FIGURE 3. Wavelet denoising procedure.

The proposed denoising procedure is as follows:

1) Select the decomposition level and wavelet basis;
2) Use DWT to decompose the signal and get the wavelet coefficients and approximated coefficients;
3) Judge the wavelet coefficient by the improved threshold T. The wavelet coefficient is marked as w' when the absolute value of the coefficient is greater

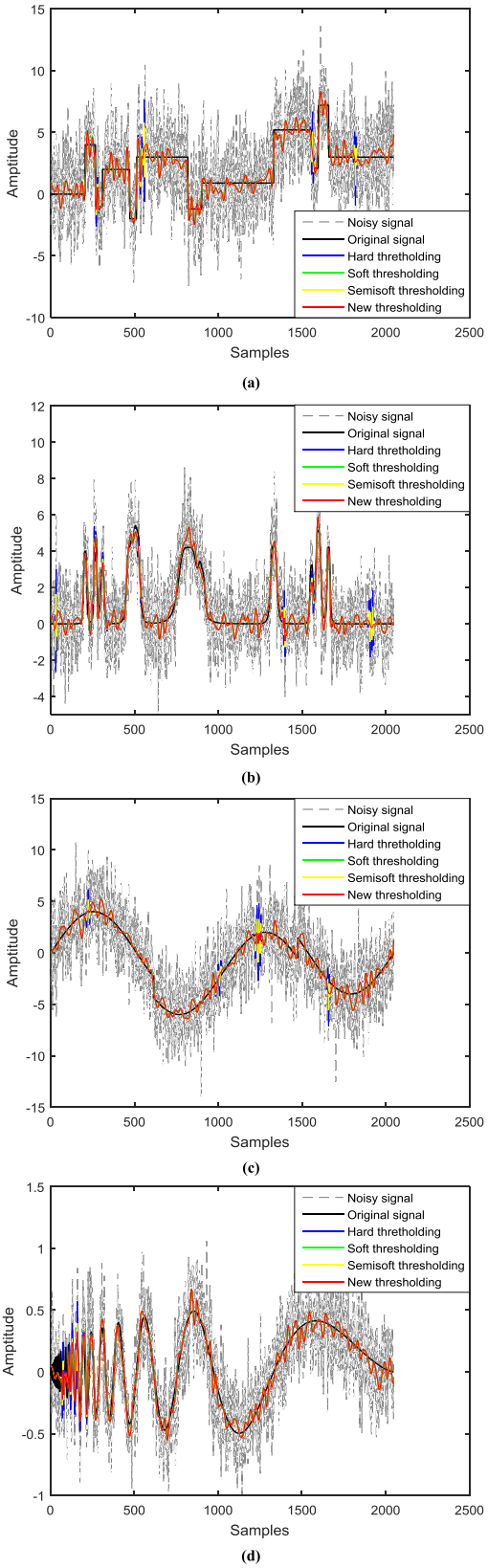

FIGURE 4. Signal denoising using four different thresholding methods (SNR≈2.0000dB), (a) Blocks signal; (b) Bumps signal; (c) Heavy sine signal; (d) Doppler signal.

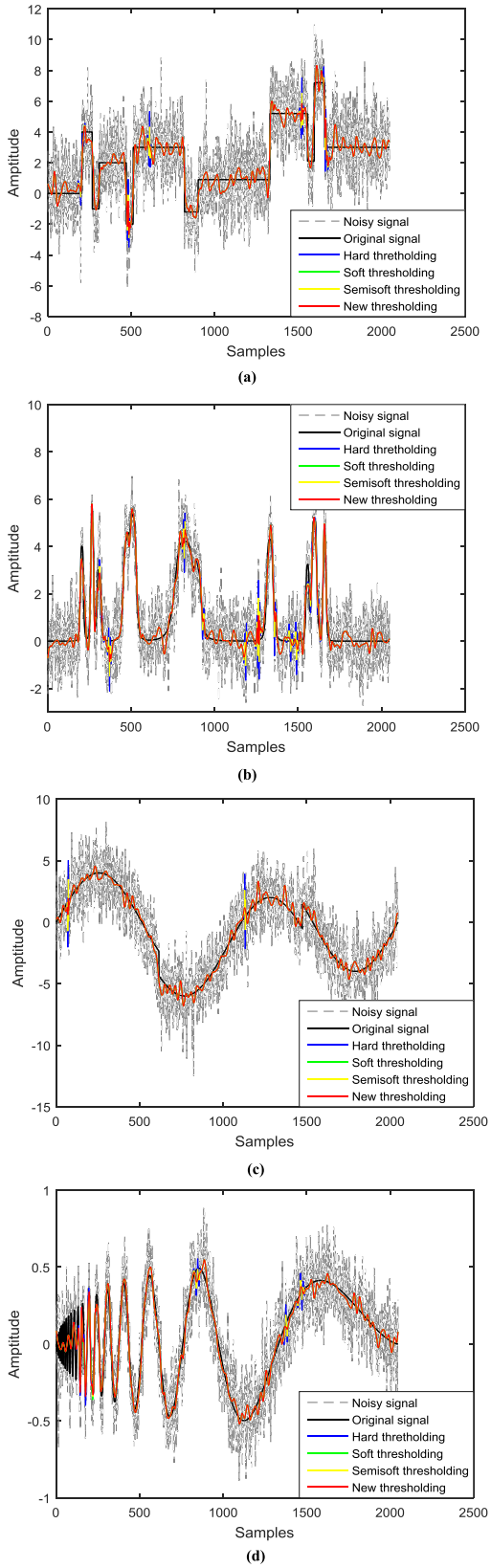

FIGURE 5. Signal denoising using four different thresholding methods (SNR≈5.0000dB), (a) Blocks signal; (b) Bumps signal; (c) Heavy sine signal; (d) Doppler signal.

than threshold T. Otherwise, the coefficient is considered w'';

4) Use estimation of inter-scale correlation to judge the coefficient when it is in $[T(1-\eta), T(1+\eta)]$. When the wavelet coefficients have a strong correlation, it is marked as w'. If it has weak correlation even no correlation, it is denoted as w''. w'' is the useful wavelet coefficient and w'' is the coefficient of noise;
5) Deal with the wavelet coefficients by the new improved thresholding function. When the coefficient is w', it should be handled with $|w| \geq T$ based on thresholding function. If the coefficient is w'', it will be set to zero according to the thresholding function that $|w| < T$;
6) Reconstruct the signal by wavelet coefficients after processing and get the denoised signal.

In the procedure, the parameter η of different value will influence the computation and accuracy of the algorithm. When the value $||w| - T|$ increases, the probability of miscalculation for the third step will decreases. So the value of η should be small. The procedure is summarized in Fig. 3.

IV. NUMERICAL SIMULATION AND ANALYSIS

A. SIMULATION SETTING

To validate the performance of the new wavelet thresholding denoising method, a simulation is conducted. In the simulation, four benchmark signals (Blocks, Bumps, Heavy Sine, Doppler) are selected as a test signal. Each signal has 2048 samples and adds three different values of SNR (near the value of 2dB, 5dB, and 10dB) on the signal. In the process, select db4 as the wavelet basis as well as the decomposition level is 4. The values of γ and η are 2 and 0.1. α is 0.6. β is 5. This paper selects five denoising methods for comparison: (1) hard thresholding function; (2) soft thresholding function; (3) semi-soft thresholding function; (4) the new thresholding function; (5) wavelet coefficient inter-scale correlation based on the new thresholding function. In order to verify the effectiveness of the proposed denoising method compared with other approaches, a number of quantitative parameters are used to measure the test results:

1) SNR (Signal to Noise Ratio)

$$SNR(dB) = 10\log\left(\frac{\sum_{i=1}^{N} x^2(i)}{\sum_{i=1}^{N}(x(i)-\widehat{x}(i))^2}\right) \tag{18}$$

Where $x(i)$ is the original signal and $\widehat{x}$ is the denoised signal. N is the number of samples composing the signal.

2) RMSE (Root mean square error)

$$RMSE = \sqrt{\frac{\sum_{i=1}^{n}\left[x(i)-\widehat{x}(i)\right]^2}{N}} \tag{19}$$

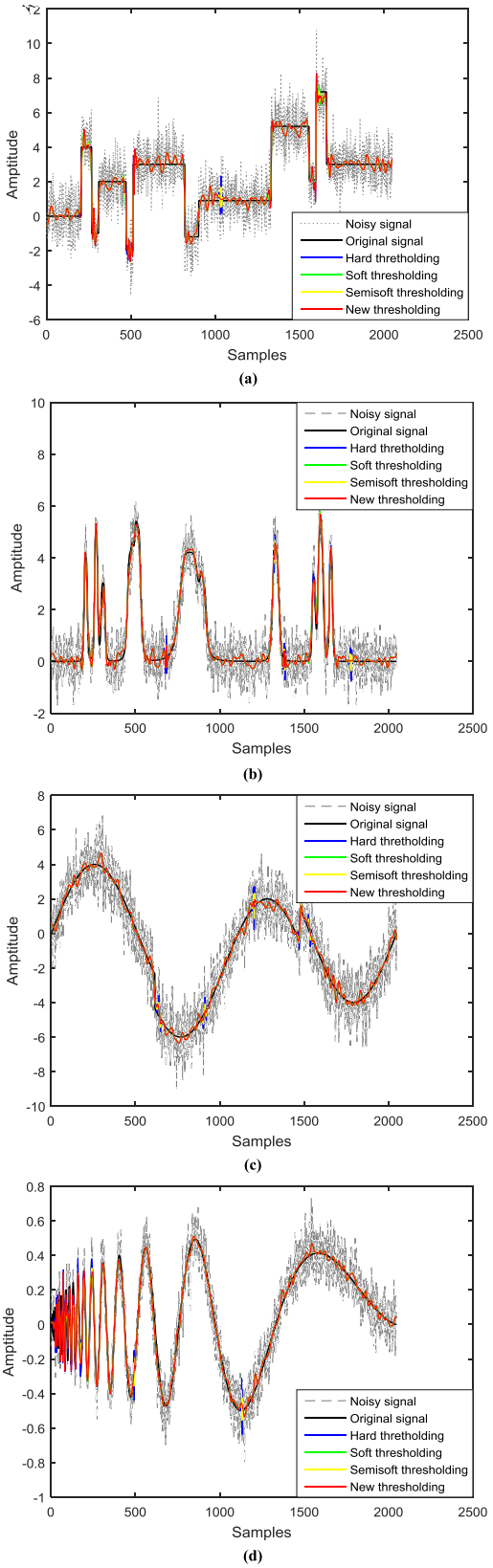

FIGURE 6. Signal denoising using four different thresholding methods (SNR≈10.0000dB), (a) Blocks signal; (b) Bumps signal; (c) Heavy sine signal; (d) Doppler signal.

TABLE 1. Performance evaluation of signals denoising with different thresholding schemes.

	Noisy signal		Hard thresholding		Soft thresholding		Semi-soft thresholding		New thresholding		Inter-scale correlation	
	SNR	RMSE	SNR	RMSE	SNR	RMSE	SNR	RMSE	SNR	RMSE	SNR	RMSE
Blocks	1.8945	2.3875	11.6438	0.7771	12.5155	0.7029	12.2806	0.7222	12.5245	0.7022	12.5330	0.7015
	4.8099	1.7068	13.6147	0.6194	13.9530	0.6194	13.9531	0.5987	13.9752	0.5942	13.9786	0.5939
	9.9347	0.9461	17.7242	0.3859	17.3830	0.4013	17.8059	0.382	17.8205	0.3816	17.8460	0.3805
Bumps	1.8585	1.4533	12.0764	0.4482	13.4109	0.3844	13.0748	0.3995	13.4201	0.3840	13.4441	0.3829
	5.0420	1.6618	13.7649	0.5365	15.4547	0.5471	14.9399	0.3223	15.4547	0.5211	15.4557	0.5201
	9.8859	0.5767	18.7082	0.2089	18.9358	0.2035	19.0893	0.1999	19.2068	0.1972	19.2088	0.1972
Heavy sine	2.0245	2.4439	12.6732	0.7172	14.0489	0.6122	13.5976	0.6448	14.0489	0.6122	14.0493	0.6121
	5.0447	1.7261	16.0426	0.4866	16.9200	0.4398	16.6355	0.4545	16.9200	0.4398	16.9208	0.4398
	9.6535	1.0154	20.3702	0.2957	21.2951	0.2658	21.0221	0.2743	21.2951	0.2658	21.2951	0.2658
Doppler	1.9835	0.2331	11.8789	0.0746	12.1533	0.0723	12.2914	0.0712	12.3375	0.0708	12.3436	0.0707
	5.1513	0.1619	14.5396	0.0549	14.7470	0.0536	14.8573	0.0530	14.9513	0.0524	14.9578	0.0523
	10.0447	0.0922	18.8161	0.0336	17.9941	0.0369	19.1799	0.0322	19.4499	0.0312	19.4549	0.0312

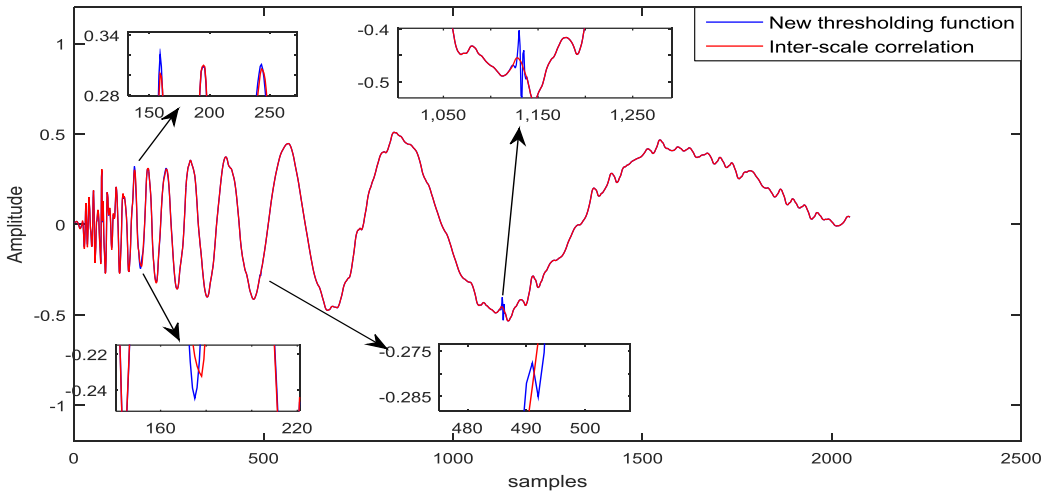

FIGURE 7. Doppler signal denoising result with the SNR at 10.000dB.

B. RESULTS AND DISCUSSION

The denoising results of four kinds of simulation signals in three different conditions are illustrated in Table 1. Two indexes can be used to measure the performance of thresholding methods: SNR and RMSE. When SNR is increasing and RMSE is decreasing, it means the performance of filtering is better. There are five denoising methods in Table 1. Compared with the noisy signal, all of the applied thresholding approaches can effectively filter the noise and improve the SNR values. The denoising performance of traditional hard/soft thresholding function is lower than the other three new thresholding schemes. The denoising method that only

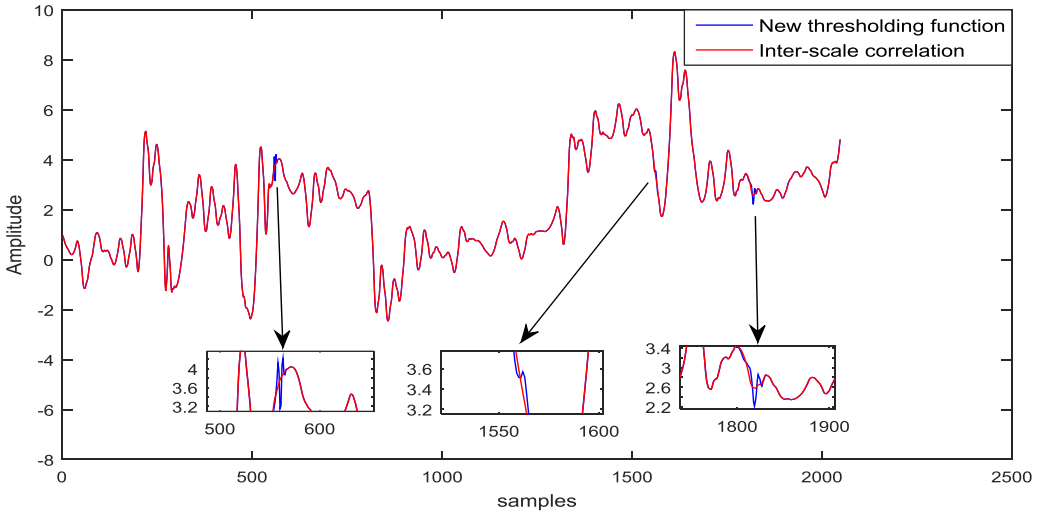

FIGURE 8. Blocks signal denoising result in the SNR at 2.000dB.

uses new thresholding function has better filtering ability than the hard/soft thresholding (at least the same). Adding the inter-scale correlation into the filtering scheme can improve the denoising effect again.

The denoising results of the noisy signal of different SNR values are shown in Fig. 4, 5 and 6, including hard/soft thresholding filtering, semi-soft thresholding filtering, and new thresholding filtering results. It is shown that the noise is effectively removed by these filtering methods. The outline of the original signal can be found clearly through the thresholding approaches whether the noise is heavy or light. In heavy noise case, the filtering schemes can remove the high noise. Moreover, in light noise case the details of the signal can be found better. The performance of the curves shows that the new thresholding method can remove some peak interference that hard thresholding couldn't eliminate from the signals. It also proves that the curve estimated by the new thresholding is closer to the original signal than the soft thresholding one. This is due to the new threshold function is adaptive and the inter-scale correlation estimation can improve the accuracy of the judgment of the wavelet coefficients near the threshold.

Fig. 7 and 8 show the different simulation results between the denoising methods based on new thresholding and inter-scale correlation. Fig. 7 shows the denoising result of Doppler signal with the SNR nearly 10.000dB and Fig. 8 shows the denoising result of Blocks signal with the SNR approximately equal to 2.000dB. The filtering results of above two figures proved that using inter-scale correlation method have better performance whether noise is high or small. It is also well shown that the improvements that reduce the peak value and remove fluctuations between the two kinds of the algorithm.

TABLE 2. Performance evaluation of signals denoising with different thresholding schemes.

	Filtering	Max	Min
Pitch angle	before	2.6046	0.2800
	after	2.5900	0.3005
Roll angle	before	1.1109	-2.2300
	after	0.7600	-1.8705
Yaw rate	before	1.8000	-2.5000
	after	0.9750	-1.9170
Heave velocity	before	0.5400	-0.4700
	after	0.2540	-0.1133
Heave acceleration	before	1.5200	-1.8800
	after	0.6694	-0.8938
Sway velocity	before	2.7600	-1.9600
	after	2.7400	-1.9015

V. HOVERCRAFT MOTION DATA PROCESSING IN SEA TRIAL

A. SEA TRIAL DATA ACQUISITION

The proposed improved wavelet thresholding and inter-scale correlation scheme with outstanding performance for denoising the signal noise has been well shown by above simulation research. Thus, this proposed scheme was applied to a certain hovercraft in sea trial and a series of experiments of hovercraft motion parameters denoising were carried out.

The six-degree-of-freedom motion (pitch, heave, roll, surge, sway, and yaw) measurement of the test hovercraft can be acquired by Fiber Optic Strapdown Compass (FOSC) with an update rate of 200Hz, including linear and angular displacement, velocity and acceleration.

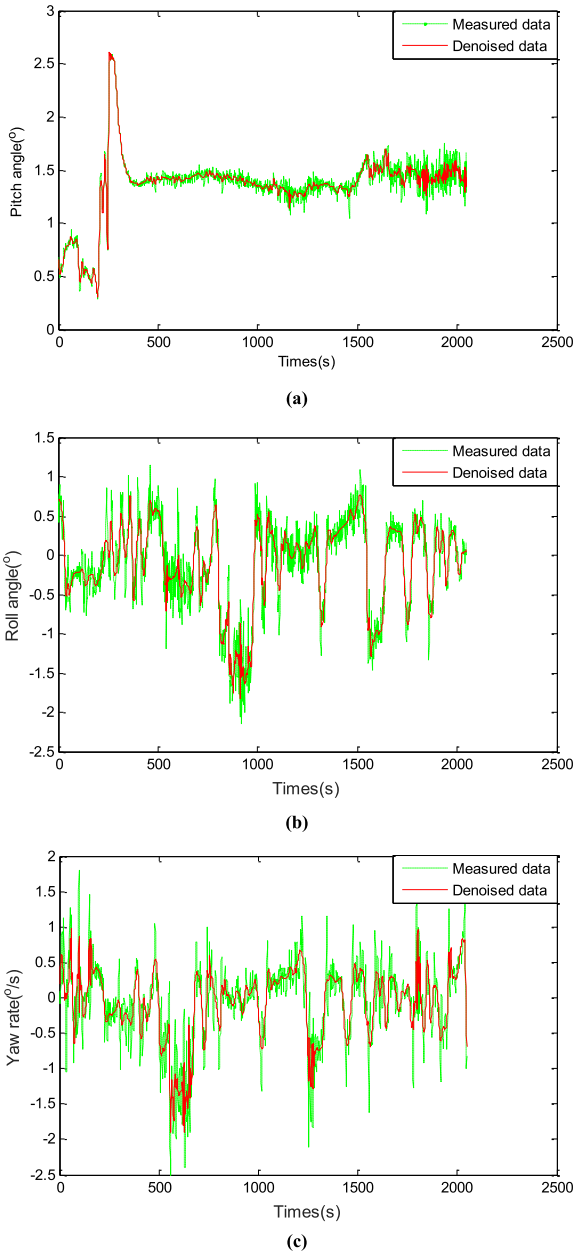

FIGURE 9. (a) Pitch angle (b) Roll angle (c) Yaw rate.

According to the maritime navigation data, the safety limits of the test hovercraft motion parameters have been defined as: Roll angle should be $0.5° \leq |\phi| \leq 2.5°$; Initial pitch angle should be $\theta \geq 0.7°$, which will normally increase with the ship speed rise, even up to $2° \sim 2.5°$; When the hovercraft sailing at the speed of 30 Knots, the yaw rate should be $|r| \leq 4°/s$ and the slide slip angle should be $|\beta| \leq 20°$ [36], [37]. It should be noted that safety limits range depends on different hovercraft and different navigation speed.

From the perspective of maneuvering safety and comfort, we select the following key parameters for data processing with a sampling rate of 1 Hz.

(i) Hovercraft safety indicator parameters (Explicit): pitch angle, roll angle, and yaw rate.

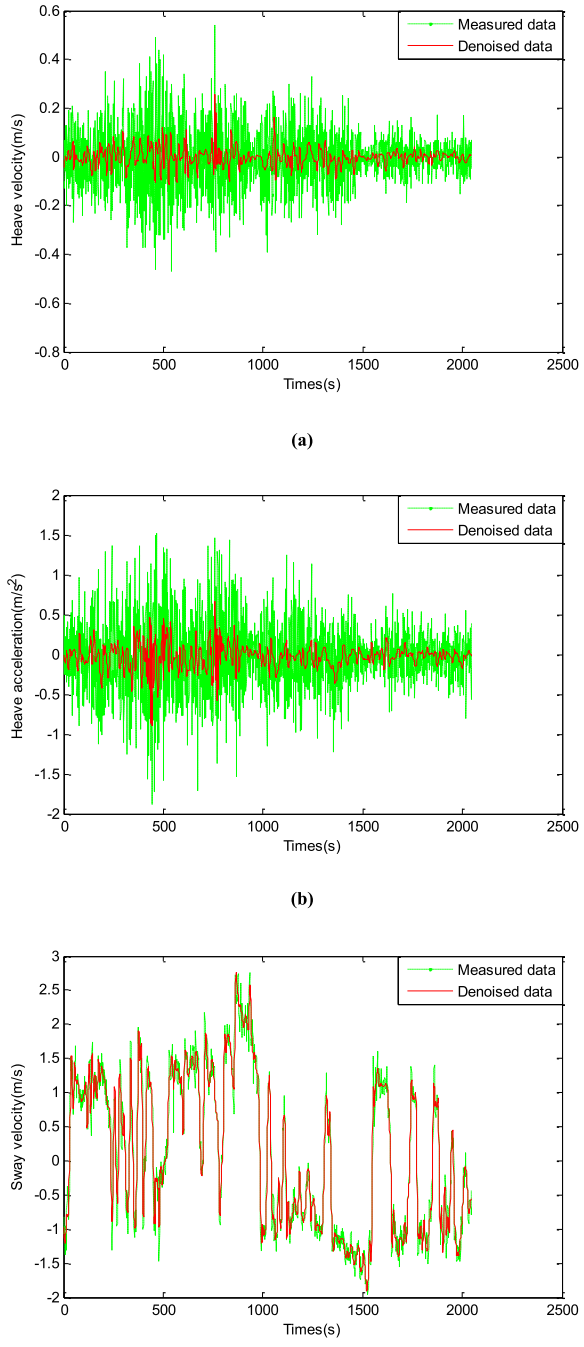

FIGURE 10. (a) Heave velocity (b) Heave acceleration (c) Sway velocity.

(ii) Hovercraft safety indicator parameters (Implicit): sway velocity, which is closely related to the slide slip angle (β). Slide slip angle is essential for active safety control systems [38].

(iii) Hovercraft comfort indicator parameters: heave velocity, heave acceleration. Where heave acceleration is the "cobblestone effect" indicator parameter. Furthermore, one would use an automatic control system to damp out some of the cobblestone effect [39].

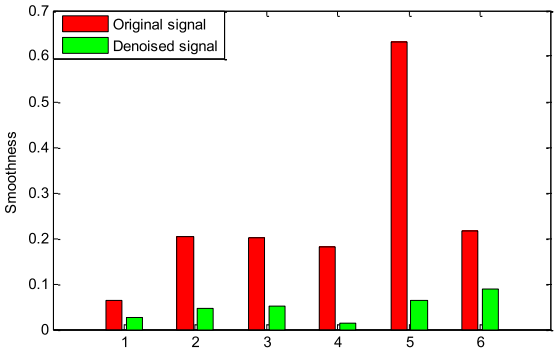

FIGURE 11. The smoothness comparison of hovercraft motion parameters between the original signal and denoised signal. (No.1: Pitch angle; No.2: Roll angle; No.3: Yaw rate; No.4: Heave velocity; No.5: Heave acceleration; No.6: Sway velocity.)

B. SEA TRIAL DATA PROCESSING

In the experiments, the hovercraft measured signals are transformed by the db4 wavelet and the wavelet decomposition level is 3. Fig. 9 and 10 shows the measured signal and denoised data. In Fig. 9 and 10, it can be observed that the measured motion parameters have high data fluctuation. The fluctuation is caused by the influence of ocean environment and hovercraft noise. If the navigation signals of hovercraft are not accurately estimated, it will affect the driver's observation and driving operation. In the sea trial, smoothness is also used to measure the test results. It is defined as:

$$R = \sqrt{\frac{\sum_{i=1}^{n} [x(i) - \bar{x}(i)]^2}{N}} \tag{20}$$

Where $x(i)$ is the value of each signal point and $\bar{x}(i)$ is the mean value of all signal point. N is the number of samples.

It can be seen from Fig. 9 and 10 that the proposed scheme can effectively reduce the fluctuation of hovercraft motion parameters (pitch angle, roll angle, yaw rate, heave velocity, heave acceleration, sway velocity) and reduce the noise in the signal. These representative parameters are carefully chosen as the most important safety and comfort indicator parameters for hovercraft navigation. The change of denoised signals can also be consistent with the corresponding original signals. From Fig.9, the well-filtered pitch angle, roll angle and yaw rate show directly that they are all within the safety limits range. From Fig. 10(b), the well-filtered heave acceleration shows the ''cobblestone effect'' is reduced to some extent. From Fig. 10(c), the well-filtered sway velocity shows indirectly the slide slip angle meet the safety limits requirements. From Table 2, it can be seen that filtering method reduces the volatility of the parameters. In Fig. 11, by calculating the smoothness of the data, we can find the smoothness is reduced apparently and the effectiveness of the proposed denoising and estimating method is effectively proved. The removal of motion parameter noise can help the driver judge the change of the hovercraft movement more accurately and improve the maneuvering safety and comfort level to a large extent.

VI. CONCLUSION

In order to remove the noise interference of dynamic motion parameters, a smoothing and estimating method is proposed in this paper. Because of traditional wavelet thresholding methods have shortcomings, a new thresholding function, an improved threshold and inter-scale correlation to estimate wavelet coefficients are used to improve the performance of denoising and estimating results. Through the numerical simulation cases study, this proposed new method is proved to effectively reduce the noise in the test signals whether the SNR is large or small and it can overcome the shortcomings of the traditional hard/soft thresholding and semi-soft thresholding algorithms.

Furthermore, the proposed improved wavelet thresholding and inter-scale correlation scheme were applied to a certain hovercraft in sea trial. Representatively, some important safety and comfort indicator parameters are selected from actual hovercraft motion measurements to verify the effect of the proposed scheme. As expected, the proposed data smoothing scheme also behaves an outstanding performance. It is shown that the proposed new scheme can decrease the fluctuation of hovercraft motion parameters and improve the effect of smoothing signal, which improves the navigation safety and comfort. Otherwise, the motion parameters closely related to safety limits and ''cobblestone effect'' can be effectively smoothed and estimated, which make the further active control be available to assure the maneuvering safety and comfort level of hovercraft navigation.

REFERENCES

[1] H. Sira-Ramirez, "Dynamic second-order sliding mode control of the hovercraft vessel," *IEEE Trans. Control Syst. Technol.*, vol. 10, no. 6, pp. 860–865, Nov. 2002.
[2] H. Seguchi and T. Ohtsuka, "Nonlinear receding horizon control of an underactuated hovercraft," *Int. J. Robust Nonlinear Control*, vol. 13, nos. 3–4, pp. 381–398, 2003.
[3] S. Yin, X. Xie, and W. Sun, "A nonlinear process monitoring approach with locally weighted learning of available data," *IEEE Trans. Ind. Electron.*, vol. 64, no. 2, pp. 1507–1516, Feb. 2017.
[4] X. Xie, W. Sun, and K. C. Cheung, "An advanced PLS approach for key performance indicator-related prediction and diagnosis in case of outliers," *IEEE Trans. Ind. Electron.*, vol. 63, no. 4, pp. 2587–2594, Apr. 2016.
[5] G. Wang, D. Li, W. Pan, and Z. Zang, "Modified switching median filter for impulse noise removal," *Signal Process.*, vol. 90, no. 12, pp. 3213–3218, 2010.
[6] K. Feser, G. Konig, J. Ott, and P. Seitz, "An adaptive filter algorithm for on-site partial discharge measurements," in *Proc. Conf. Rec. IEEE Int. Symp. Elect. Insul.*, Jun. 1988, pp. 242–245.
[7] A. G. Constantinides and B. Baykal, "A neural approach to the underdetermined-order recursive least-squares adaptive filtering" *Neural Netw.*, vol. 10, no. 8, pp. 1523–1531, 1997.
[8] U. Kopf and K. Feser, "Rejection of narrow-band noise and repetitive pulses in on-site PD measurements," *IEEE Trans. Dielectr. Electr. Insul.*, vol. 2, no. 3, pp. 433–446, Jun. 1995.
[9] S. Yin and X. Zhu, "Intelligent particle filter and its application to fault detection of nonlinear system," *IEEE Trans. Ind. Electron.*, vol. 62, no. 6, pp. 3852–3861, Jun. 2015.
[10] D. L. Donoho and I. M. Johnstone, "Adapting to unknown smoothness via wavelet shrinkage," *J. Amer. Statist. Assoc.*, vol. 90, no. 432, pp. 1200–1224, 1995.
[11] P. Ray, A. K. Maitra, and A. Basuray, "A new threshold function for de-noising partial discharge signal based on wavelet transform," in *Proc. Int. Conf. Signal Process. Image Process. Pattern Recognit.*, 2013, pp. 185–189.

[12] M. Han, Y. Liu, J. Xi, and W. Guo, "Noise smoothing for nonlinear time series using wavelet soft threshold," *IEEE Signal Process. Lett.*, vol. 14, no. 1, pp. 62–65, Jan. 2007.
[13] S. Hosur and A. H. Tewfik, "Wavelet transform domain adaptive FIR filtering," *IEEE Trans. Signal Process.*, vol. 45, no. 3, pp. 617–630, Mar. 1997.
[14] Z. Huo, Y. Zhang, P. Francq, L. Shu, and J. Huang, "Incipient fault diagnosis of roller bearing using optimized wavelet transform based multi-speed vibration signatures," *IEEE Access*, vol. 5, pp. 19442–19456, 2017.
[15] M. Abo-Zahhad, A. F. Al-Ajlouni, S. M. Ahmed, and R. J. Schilling, "A new algorithm for the compression of ECG signals based on mother wavelet parameterization and best-threshold levels selection," *Digit. Signal Process.*, vol. 23, no. 3, pp. 1002–1011, 2013.
[16] D. L. Donoho and J. M. Johnstone, "Ideal spatial adaptation by wavelet shrinkage," *Biometrika*, vol. 81, no. 3, pp. 425–455, 1994.
[17] H.-Y. Gao, "Wavelet shrinkage denoising using the non-negative garrote," *J. Comput. Graph. Statist.*, vol. 7, no. 4, pp. 469–488, 1998.
[18] A. C. To, J. R. Moore, and S. D. Glaser, "Wavelet denoising techniques with applications to experimental geophysical data," *Signal Process.*, vol. 89, no. 2, pp. 144–160, 2009.
[19] S. Bacchelli and S. Papi, "Filtered wavelet thresholding methods," *J. Comput. Appl. Math.*, vols. 164–165, no. 1, pp. 39–52, 2004.
[20] T.-H. Yi, H.-N. Li, and X.-Y. Zhao, "Noise smoothing for structural vibration test signals using an improved wavelet thresholding technique," *Sensors*, vol. 12, no. 8, pp. 11205–11220, 2012.
[21] C. He, J. Xing, J. Li, Q. Yang, and R. Wang, "A new wavelet thresholding function based on hyperbolic tangent function," *Math. Problems Eng.*, vol. 2015, Sep. 2015, Art. no. 528656.
[22] J.-Y. Lu, H. Lin, D. Ye, and Y.-S. Zhang, "A new wavelet threshold function and denoising application," *Math. Problems Eng.*, vol. 2016, May 2016, Art. no. 3195492.
[23] R. Hussein, K. B. Shaban, and A. H. El-Hag, "Wavelet transform with histogram-based threshold estimation for online partial discharge signal denoising," *IEEE Trans. Instrum. Meas.*, vol. 64, no. 12, pp. 3601–3614, Dec. 2015.
[24] S. Lee and J. Kim, "Discrete wavelet transform-based denoising technique for advanced state-of-charge estimator of a lithium-ion battery in electric vehicles," *Energy*, vol. 83, pp. 462–473, Apr. 2015.
[25] S. Badiezadegan and R. C. Rose, "A wavelet-based thresholding approach to reconstructing unreliable spectrogram components," *Speech Commun.*, vol. 67, pp. 129–142, Mar. 2015.
[26] K. Mcginnity, R. Varbanov, and E. Chicken, "Cross-validated wavelet block thresholding for non-Gaussian errors," *Comput. Statist. Data Anal.*, vol. 106, pp. 127–137, Feb. 2017.
[27] S. Yin, X. Xie, J. Lam, K. C. Cheung, and H. Gao, "An improved incremental learning approach for KPI prognosis of dynamic fuel cell system," *IEEE Trans. Cybern.*, vol. 46, no. 12, pp. 3135–3144, Dec. 2016.
[28] A. K. Bhandari, D. Kumar, A. Kumar, and G. K. Singh, "Optimal sub-band adaptive thresholding based edge preserved satellite image denoising using adaptive differential evolution algorithm," *Neurocomputing*, vol. 174, pp. 698–721, Jan. 2016.
[29] X. J. Chen, W. T. Wang, M. C. Jia, and N. Song, "New de-noising method for speech signal based on wavelet entropy and adaptive threshold," *Appl. Res. Comput.*, vol. 12, no. 3, pp. 1257–1265, 2015.
[30] T. F. Sanam and C. Shahnaz, "Noisy speech enhancement based on an adaptive threshold and a modified hard thresholding function in wavelet packet domain," *Digit. Signal Process.*, vol. 23, no. 3, pp. 941–951, 2013.
[31] S. Tabibian, A. Akbari, and B. Nasersharif, "Speech enhancement using a wavelet thresholding method based on symmetric Kullback–Leibler divergence," *Signal Process.*, vol. 106, pp. 184–197, Jan. 2015.
[32] A. P. Witkin, "Scale-space filtering," *Readings Comput. Vis.*, vol. 42, no. 3, pp. 329–332, 1987.
[33] S. Mallat and W. L. Hwang, "Singularity detection and processing with wavelets," *IEEE Trans. Inf. Theory*, vol. 38, no. 2, pp. 617–643, Mar. 1992.
[34] Y. Xu, J. B. Weaver, D. M. Healy, and J. Lu, "Wavelet transform domain filters: A spatially selective noise filtration technique," *IEEE Trans. Image Process.*, vol. 3, no. 6, pp. 747–758, Nov. 1994.
[35] Y. Zheng, D. B. H. Tay, and L. Li, "Signal extraction and power spectrum estimation using wavelet transform scale space filtering and Bayes shrinkage," *Signal Process.*, vol. 80, no. 8, pp. 1535–1549, 2000.
[36] F. Ding *et al.*, "Judgment method of safety boundary of hovercraft," Google Patents 105 184 001 A, Dec. 23, 2015.
[37] L. Zhang, "Research on safety navigation control strategy method for air cushion vehicle," (in Chinese), Ph.D. dissertation, Dept. College Autom., Harbin Eng. Univ., Harbin, China, 2015.
[38] J. Li and J. Zhang, "Vehicle sideslip angle estimation based on hybrid Kalman filter," *Math. Problems Eng.*, vol. 2016, Jun. 2016, Art. no. 3269142.
[39] O. M. Faltinsen, *Hydrodynamics of High-Speed Marine Vehicles*. Cambridge, U.K.: Cambridge Univ. Press, 2005.

YUANHUI WANG received the B.S., M.S., and Ph.D. degrees from Harbin Engineering University, Harbin, China. She is currently an Associate Professor with the College of Automation, Harbin Engineering University. She is also a Post-Doctoral Research Fellow with the Department of Biomedical Engineering, National University of Singapore, Singapore. Her research interests include guidance, navigation and control of marine crafts, ship dynamic positioning, ship dynamics and motion control, robot path planning, signal processing, and surgical robotics motion planning.

BO ZHANG received the M.S. degree from Harbin Engineering University, Harbin, China, where he is currently pursuing the master's degree with the College of Automation. His research interests include signal processing and ship motion control.

FUGUANG DING received the M.S. degree from Harbin Engineering University, Harbin, China. He is currently a Professor with the College of Automation, Harbin Engineering University. His research interests include ship motion control, ship dynamic positioning, hardware-in-loop simulation technique, and embedded system application.

HONGLIANG REN (SM'17) received the Ph.D. degree in electronic engineering (specialized in biomedical engineering) from The Chinese University of Hong Kong in 2008. He was a Research Fellow with The Johns Hopkins University, Children's Hospital Boston and Harvard Medical School, and Children's National Medical Center, USA. He is currently an Assistant Professor and leading a Research Group on medical mechatronics with the Biomedical Engineering Department, National University of Singapore (NUS). He is an affiliated Principal Investigator with the Singapore Institute of Neurotechnology (SINAPSE), NUS Research Institute, Suzhou, and Advanced Robotics Center, NUS. His main areas of interests include biorobotics and intelligent control, medical mechatronics, computer-integrated surgery, and multisensor data fusion in surgical robotics. He serves as an Associate Editor for the IEEE Transactions on Automation Science and Engineering and the *Medical and Biological Engineering and Computing*. He was a recipient of the IAMBE Early Career Award 2018.